Composites Communications 12 (2019) 117–122

Contents lists available at ScienceDirect

Composites Communications

journal homepage: www.elsevier.com/locate/coco

Short Communication

Assembly of 2D graphene sheets and 3D carbon nanospheres into flexible composite electrodes for high-performance supercapacitors

Zhaoqi Huang, Hele Guo, Chao Zhang*

State Key Laboratory for Modification of Chemical Fibers and Polymer Materials, College of Materials Science and Engineering, Innovation Center for Textile Science and Technology, Donghua University, 2999 North Renmin Road, Shanghai, 201620, PR China

ARTICLE INFO

Keywords:
Graphene
Hydrothermal carbon nanospheres
Vacuum filtration
Supercapacitors

ABSTRACT

Flexible paper electrodes with high conductivity and hierarchical porosity have been intensely required to develop next-generation supercapacitors with high energy density and power density. Herein, glucose-derived hydrothermal carbon nanospheres (CNSs) are chemically activated into highly porous carbon nanospheres (HPCNSs), which are uniformly dispersed by graphene oxide (GO) in water. Upon filtration, the resultant GO/HPCNS composites are assembled into a flexible composite paper of HPCNSs embedded in a parallelly arranged GO framework. Upon chemical reduction from GO to reduced graphene oxide (rGO), the rGO/HPCNS composite paper as a binder-free electrode facilitates the assembly of flexible supercapacitors. The rGO/HPCNS composite paper with optimized rGO/HPCNS ratio delivers high specific capacitance (235.3 F g^{-1} at 0.2 A g^{-1}) and high cyclic stability (capacitance retention of 91% at 5 A g^{-1} after 5000 charge/discharge cycles), attributing to their excellent structural stability, 3D conductive network and hierarchical porosity.

1. Introduction

Due to the depletion of fossil fuel supplies, energy shortage has become one of the most important issues recently. Among existing energy storage devices, due to their high power density, long lifetime and low maintenance cost, supercapacitors offer a promising approach to meet increasing demands of promising energy storages [1–4]. To make breakthroughs in critical technologies for the developments of supercapacitors, the design and synthesis of high-performance electrode materials unquestionably provides important and efficient routes for largely improving the electrochemical performance of as-fabricated supercapacitors [5]. Carbon materials and their composites are intensively investigated as high-performance electrode materials in the past years [6–9]. Carbon composites, a family of new-emerging advanced composite materials mainly including carbon materials such as carbon nanotubes, graphene, and carbon nanospheres (CNSs), have attracted considerable attention due to their tunable graphitic structures and tailored properties far beyond individual carbon materials. For instance, the combination of graphene and CNSs into hierarchical carbon composites has been achieved for energy storage [7,8]. With well-designed nanostructures, individual CNSs were wrapped with graphene sheets, and thus large enhancements in electrochemical performance have been observed due to efficient ion/electron transports in the composites.

At present, the challenges still remain in the preparation of hierarchical carbon composites. One is how to achieve an enhanced interaction between individual carbon materials throughout the composites, and the other one is how to obtain ordered nanostructures in a macroscopic scale [10,11]. To address these issues, we described a simple and efficient strategy for the fabrication of a carbon composite paper consisting of two-dimensional (2D) reduced graphene oxide (rGO) and three-dimensional (3D) highly porous carbon nanospheres (HPCNSs) via filtration-induced self-assembly followed by chemical reduction. The 2D rGO and 3D HPCNSs were assembled into mechanically flexible, electrically conductive and lightweight paper-like materials. The resultant carbon composite paper with a tunable rGO-to-HPCNS ratio as a self-standing electrode material for supercapacitors shows largely improved capacitances than that of neat rGO paper. This study thus provides a straightforward strategy for the preparation of flexible and ordered carbon composite paper with nanocarbon building blocks in different dimensions, and their practical applications as flexible supercapacitor electrodes are also demonstrated.

2. Results and discussion

The CNSs were synthesized via a hydrothermal carbonization from glucose according to literature [12,13]. The as-obtained CNSs were further chemically activated using potassium hydroxide (KOH) to

* Corresponding author.
E-mail address: czhang@dhu.edu.cn (C. Zhang).

https://doi.org/10.1016/j.coco.2019.01.010
Received 18 December 2018; Received in revised form 23 January 2019; Accepted 31 January 2019
Available online 01 February 2019

generate the HPCNSs with well-defined micropores [14]. TEM images of the CNSs and HPCNSs (Figs. S1a–1b) indicate that the HPCNSs maintain the spherical shapes but show higher surface roughness after activation. Figs. S2c and 2d show the nitrogen adsorption/desorption isotherms and corresponding pore size distributions of the CNSs and HPCNSs. Different from the CNSs with almost no nitrogen adsorptions, the HPCNSs show much larger nitrogen adsorption ability. The nitrogen adsorption isotherms of the HPCNSs are almost type I, indicating that the HPCNSs have large micropore volumes [15]. The summarized data in Table S1 indicates that the HPCNSs exhibit a large surface area of 887 $m^2 g^{-1}$ with pore sizes smaller than 8 Å, suggesting the successful introduction of micropores into CNSs via KOH activation.

A non-covalent strategy for the uniform dispersion of HPCNSs using GO as the dispersants was further proposed, thus forming a carbon composite of GO and HPCNSs [16–18]. Fig. S3 shows an atomic force microscope (AFM) image and height profile of the GO sheets. The GO sheets show a uniform thickness of 1.1–1.3 nm, and the lateral sizes are in a range of several to several dozens of micrometers. A uniform suspension of the GO/HPCNS composites was simply prepared by adding the HPCNSs into the GO suspension (2 mg mL^{-1}) under sonication for half an hour. Fig. 1a illustrates the aqueous dispersibility of the GO, GO/HPCNS-2 and HPCNSs after settling for two days. The dispersion of the GO is pretty good, while serious precipitation is observed for the HPCNSs. For the case of the GO/HPCNS-2, no precipitation is found at the bottom of the vial. TEM observations also indicate an efficient composition evidences for 2D GO sheets and 3D HPCNSs. Fig. 1b shows the TEM image of the GO/HPCNS-2, indicating that the GO sheets are separated with closely packaged HPCNSs. No obvious aggregations of individual HPCNSs and GO are observed. Therefore, the GO sheets serve as 2D dispersant for uniformly dispersing the HPCNSs due to close interactions between the GO sheets and HPCNSs (Fig. 1c).

The aqueous dispersion of the GO/HPCNS composites fascinates the fabrication of GO-based composite papers [19–23]. As shown in Fig. 2, the GO/HPCNS composites as the building blocks were vacuum filtered, forming a pressure-induced orientation of GO within the resultant composite papers. The thicknesses of the GO/HPCNS composite papers were simply controlled by tuning the amounts of the GO/HPCNS composites for filtration. Upon drying at 60 °C overnight, a free-standing GO/HPCNS composite paper was obtained. The GO/HPCNS composite papers with 4/1, 2/1 and 1/1 GO/HPCNS ratios show a good flexibility. However, upon further increasing the HPCNS contents, the composite papers typically became brittle, which were easily broken

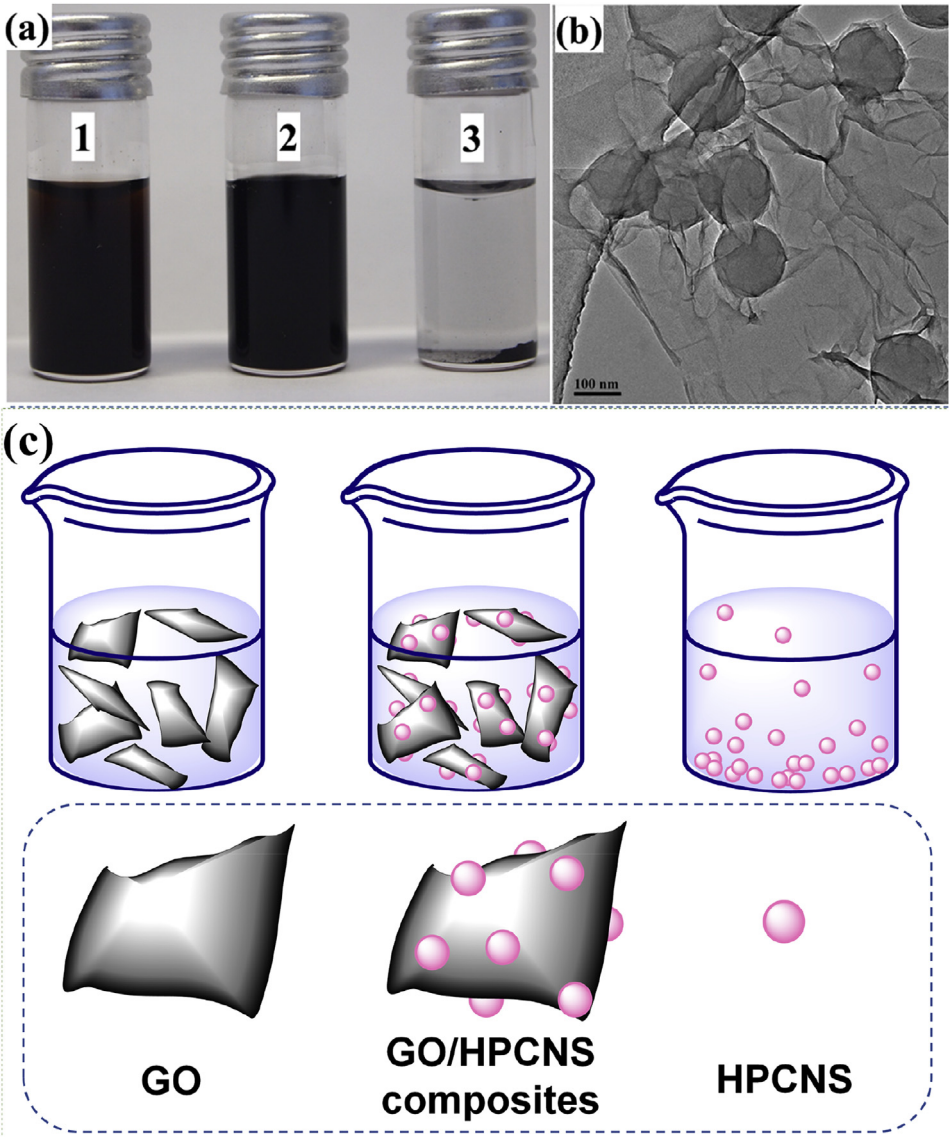

Fig. 1. (a) Digital picture showing the dispersion of GO, GO/HPCNS-2, and HPCNSs in water. (b) TEM image of GO/HPCNS-2. (c) Schematic illustration for the assisted-dispersion of HPCNSs using GO sheets.

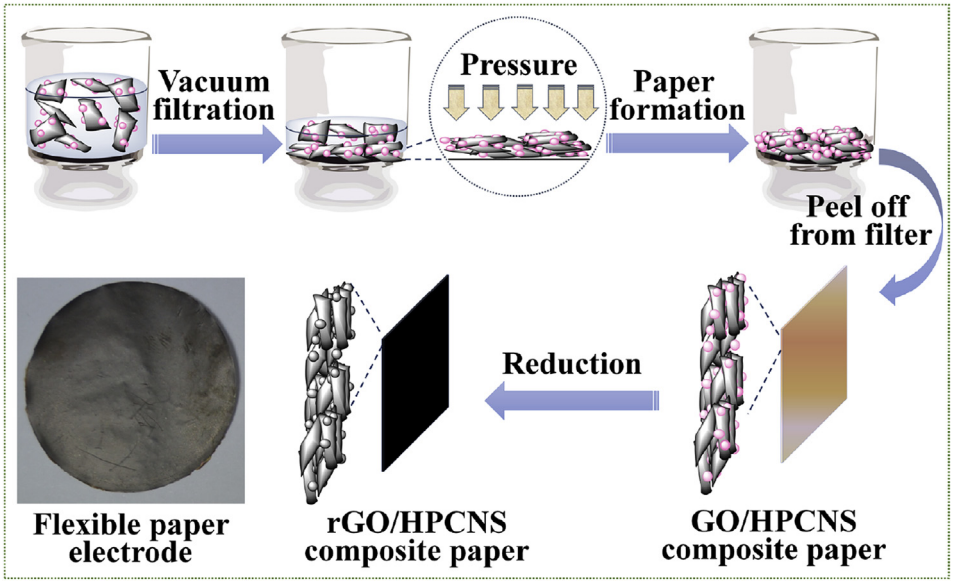

Fig. 2. Schematic illustration for the fabrication of the flexible rGO/HPCNS composite papers.

upon drying. The GO sheets within the GO/HPCNS composite papers were then chemically reduced into rGO using hydroiodic acid (HI) as the reducing agent, and the good flexibility of the rGO/HPCNS composite papers still maintained. The Raman spectra of the GO and rGO show that the I_D/I_G ratios increase significantly from 1.04 to 1.41 (Fig. S4), indicating the successful reduction of GO [24].

Fracture-surface SEM images of the rGO/HPCNS composite papers were obtained (Fig. 3). All the samples clearly show a highly-ordered aligned structure, indicating that arranged rGO assemblies were achieved under the directional filtration flow. The HPCNSs bridged the space between the large lateral rGO framework, and additional pores surrounding the HPCNSs were obtained.

Fig. 4a and b indicate the nitrogen adsorption isotherms and pore size distributions of neat rGO and rGO/HPCNS composite papers (summarized in Table 1). Neat rGO paper shows a low surface area of 67 $m^2 g^{-1}$, and the pore sizes are mainly micropores. With addition of the HPCNSs into the rGO interlayers, the surface area of the composite papers dramatically increases into 170, 496 and 460 $m^2 g^{-1}$ for the rGO/HPCNS-1, rGO/HPCNS-2 and rGO/HPCNS-3, respectively. More interestingly, the mesoporous structures are successfully introduced into the composite papers, for instances, the proportion of the micropore volume of the rGO/HPCNS-2 increases into 41%. The hierarchical porosity among the rGO/HPCNS-2 composite paper fascinates an efficient ion transfer during electrochemical processes [25].

Fig. S5a shows the CV curves of the CNSs and HPCNSs in a 1 M H_2SO_4 electrolyte, while Fig. S5b exhibits the specific capacitances of the CNSs and HPCNSs at various current densities. The HPCNSs show a much larger capacitance than that of neat CNSs. The dramatic decreases of capacitances of the HPCNSs especially under large current density attribute to micropores-only structure presenting limited ion accessibility [26]. Fig. 5a shows the CV curves of the rGO and rGO/HPCNS composite papers in acidic electrolyte, and Fig. 5b summaries

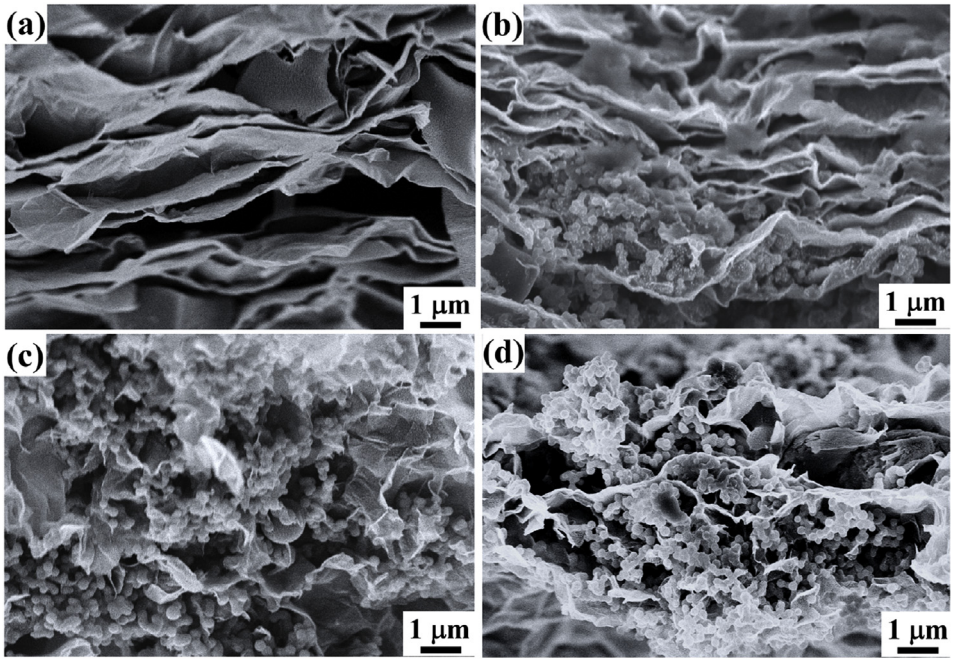

Fig. 3. Cross-section SEM images of (a) rGO, (b) rGO/HPCNS-1, (c) rGO/HPCNS-2 and (d) rGO/HPCNS-3 composite papers.

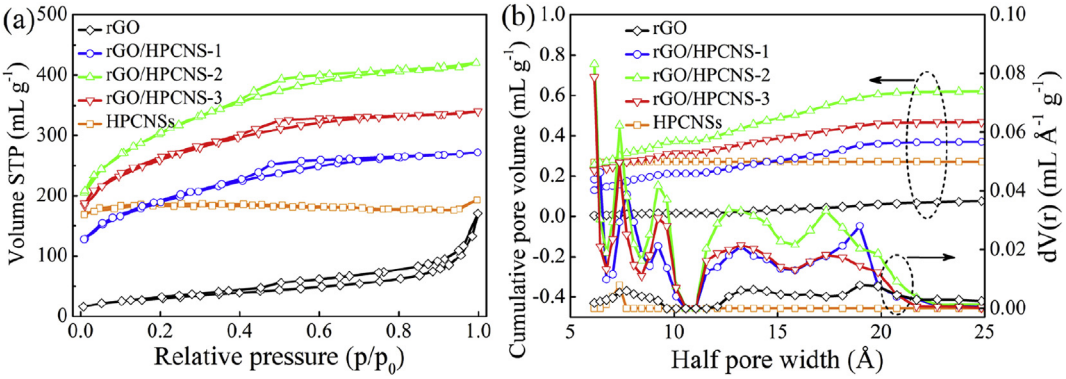

Fig. 4. (a) Nitrogen adsorption-desorption isotherms and (b) pore size distributions of the rGO, rGO/HPCNS-1, rGO/HPCNS-2, rGO/HPCNS-3 and HPCNSs.

Table 1
BET surface areas and pore size distributions of rGO and rGO/HPCNS composite papers.

Sample	S_{BET} [$m^2\ g^{-1}$]	Pore volume [$mL\ g^{-1}$]		
		Total	Micro	Meso
rGO	67	0.09	0.08	0.01
rGO/HPCNS-1	170	0.10	0.05	0.05
rGO/HPCNS-2	496	0.22	0.13	0.09
rGO/HPCNS-3	460	0.19	0.13	0.06

the specific capacitances of these electrodes at different current densities. The CV curves show the rectangular shapes ascribing to the electric double-layer capacitor (EDLC) behaviors. The specific capacitances of the rGO/HPCNS composite papers are far superior to that of neat rGO paper. In particular, the specific capacitance of the rGO/HPCNS-2 (235.5 F g^{-1}) at 0.2 A g^{-1} is notably higher than that of neat rGO (135.5 F g^{-1}). The specific capacitance of the rGO/HPCNS-2 reaches 130 F g^{-1} at 10 A g^{-1}, maintaining a 55% of the capacitance at 0.2 A g^{-1}. Table S2 compares the electrochemical performance of rGO/HPCNS-2 composite paper electrode with recently-reported graphene-based films for supercapacitors. The results indicate that the rGO/HPCNS-2 composite paper is a promising electrode material for supercapacitors. The excellent rate capabilities are ascribed to largely improved ionic conductivities of the composite papers, and the extremely stable 3D rGO/HPCNS-2 composite framework contributes well for the high rate performance [4].

The rGO/HPCNS-2 composite paper exhibits an excellent capacitive property in ranges of scan rates of 20–500 mV s^{-1} in Fig. 5c, and the increased current densities with increased scan rates mean their excellent rate capabilities for the rGO/HPCNS electrodes. The shapes of the CV curves of the electrodes remain undistorted at an extremely large scan rate of 500 mV s^{-1}. The cycling data of rGO/HPCNS composite papers and neat rGO paper are presented in Fig. 5d. The specific capacitance of the rGO/HPCNS-2 electrode maintains at 142.9 F g^{-1} after 5000 charge/discharge cycles, which is much higher than that of rGO (82.8 F g^{-1}), rGO/HPCNS-1 (132.5 F g^{-1}) and rGO/HPCNS-3 (90.3 F g^{-1}), demonstrating its favorable cycling stability. Electrochemical impedance spectroscopy (EIS) is used to investigate the transport behaviors of the electrodes, and the resultant Nyquist plots are shown in Fig. 5e. First, in low-frequency regions, vertical lines of the impedance plots are the characteristics of pure EDLC behaviors. The Nyquist plots of the rGO paper and rGO/HPCNS composite papers show relatively vertical lines in low-frequency region, and vertical shapes at low-frequency region indicate their ion-diffusion-controlled behaviors within the electrodes. Second, the intercepts of the EIS curves at X-axis at high-frequency region represent the equivalent series resistance (R_s) of the electrodes. The rGO and rGO/HPCNS composite papers show the R_s values at ~5.5 Ω, indicating a good conducting nature of the electrodes. The diameters of the semicircles in high-frequency region indicate the charge transfer resistance (R_{ct}) of the electrodes, and the R_{ct} values of the rGO, rGO/HPCNS-1 and rGO/HPCNS-2 exhibit similar small values. Therefore, the excellent electron/ion diffusion behaviors result in good electrochemical performance of the rGO/HPCNS-2 electrodes.

A possible mechanism for largely enhanced capacitive performance for the composite paper electrodes was thus proposed (Fig. 5f). First, the capacitive enhancements were ascribed to smaller resistances and rapider electron transport pathways within the electrodes, because imbedded HPCNSs acted as novel “crosslinking” sites bridging parallelly arranged rGO sheets into a highly conductive framework [27], which was also confirmed by the enhanced conductivity from the EIS results (Fig. 5e). Second, the significantly improved capacitances of the rGO/HPCNS composite electrodes were ascribed to unique hierarchical porosity, namely, besides the micropores within the HPCNSs, the introduction of hierarchical structures throughout the composite papers contributed to more efficient ionic transport [28]. Moreover, mechanical flexibility of the composite papers were another important reason for the largely improved capacitive performance [29].

3. Conclusion

In summary, a simple and practical strategy of vacuum-assisted self-assembly has been used to fabricate flexible and electrically conductive carbon composite papers. The resultant rGO/HPCNS composite papers show much improved electrochemical performance than that of neat rGO paper. The well-designed and uniform-distributed meso- and micro-pores within the rGO/HPCNS composite papers play significant roles in improving the capacitive behaviors including a high specific capacitance (235.3 F g^{-1} at 0.2 A g^{-1}) and good cycle performance (a capacitance retention of 91% at 5 A g^{-1} after 5000 charge/discharge cycles). This study therefore proposed a simple and effective way to fabricate unique carbon composite paper-like materials to meet their diverse applications in energy fields such as flexible batteries, solar cells and sensors.

Acknowledgements

This work was supported by the National Natural Science Foundation of China (21504012 and 51773035) the Natural Science Foundation of Shanghai (17ZR1439900), and the Shanghai Scientific and Technological Innovation Project (18JC1410600).

Appendix A. Supplementary data

Supplementary data to this article can be found online at https://doi.org/10.1016/j.coco.2019.01.010.

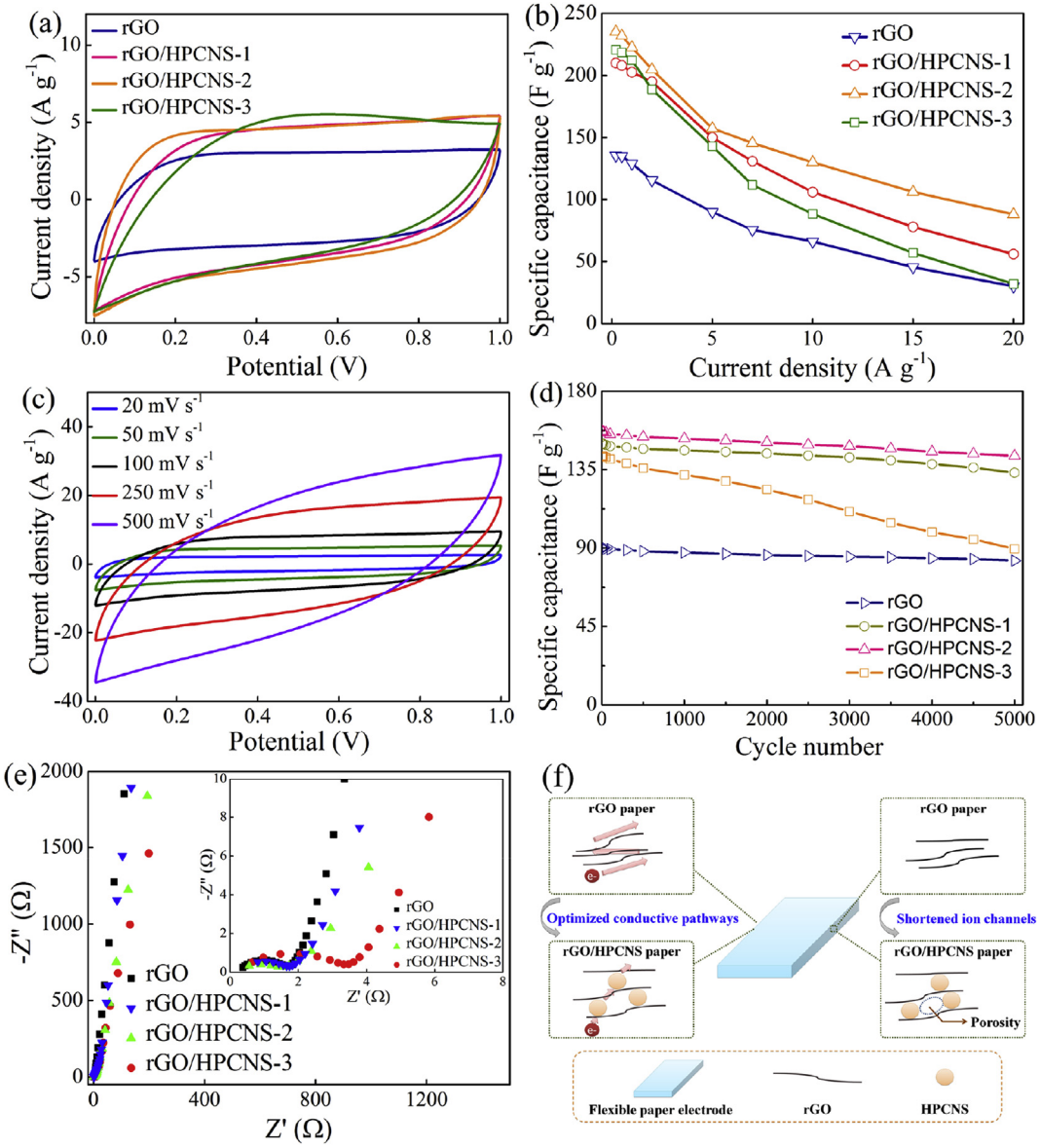

Fig. 5. (a) CV curves of the rGO, rGO/HPCNS-1, rGO/HPCNS-2, rGO/HPCNS-3 at 20 mV s^{-1}. (b) Specific capacitances of the rGO, rGO/HPCNS-1, rGO/HPCNS-2, rGO/HPCNS-3 as a function of current densities. (c) CV curves of the rGO/HPCNS-2 electrode at different scan rates. (d) Cycling performance of neat rGO and rGO/HPCNS composite paper electrodes at 5 A g^{-1}. (e) EIS (inset: magnified region) of rGO and rGO/HPCNS composite papers at open circuit potential. (f) Schematic illustration for the capacitive enhancements of the rGO/HPCNS composite papers.

References

[1] K.J. Stevenson, V. Ozolins, B. Dunn, Electrochemical energy storage, Acc. Chem. Res. 46 (2013) 1051–1052.

[2] P. Simon, Y. Gogotsi, Capacitive energy storage in nanostructured carbon-electrolyte systems, Acc. Chem. Res. 46 (2013) 1094–1103.

[3] L.L. Zhang, X.S. Zhao, Carbon-based materials as supercapacitor electrodes, Chem. Soc. Rev. 38 (2009) 2520–2531.

[4] Z. Huang, L. Li, Y. Wang, C. Zhang, T.X. Liu, Polyaniline/graphene nanocomposites towards high-performance supercapacitors: a review, Compos. Commun. 8 (2018) 83–91.

[5] Y. Yamada, T. Sasaki, N. Tatsuda, D. Weingarth, K. Yano, R. Kötz, A novel model electrode for investigating ion transport inside pores in an electrical double-layer capacitor: monodispered microporous starburst carbon spheres, Electrochim. Acta 81 (2012) 138–148.

[6] Z. Fan, J. Yan, L. Zhi, Q. Zhang, T. Wei, J. Feng, et al., A three-dimensional carbon nanotube/graphene sandwich and its application as electrode in supercapacitors, Adv. Mater. 22 (2010) 3723–3728.

[7] C.X. Guo, C.M. Li, A self-assembled hierarchical nanostructure comprising carbon spheres and graphene nanosheets for enhanced supercapacitor performance, Energy Environ. Sci. 4 (2011) 4504–4507.

[8] Z.B. Lei, N. Christov, X.S. Zhao, Intercalation of mesoporous carbon spheres between reduced graphene oxide sheets for preparing high-rate supercapacitor electrodes, Energy Environ. Sci. 4 (2011) 1866–1873.

[9] X. Li, Y. Tang, J. Song, W. Yang, M. Wang, C. Zhu, et al., Self-supporting activated carbon/carbon nanotube/reduced graphene oxide flexible electrode for high performance supercapacitor, Carbon 129 (2018) 236–244.

[10] L. Huang, D. Santiago, P. Loyselle, L. Dai, Graphene-based nanomaterials for flexible and wearable supercapacitors, Small 14 (2018) 1800879.

[11] Y. Wang, X. Yang, L. Qiu, D. Li, Revisiting the capacitance of polyaniline by using graphene hydrogel films as a substrate: the importance of nano-architecturing, Energy Environ. Sci. 6 (2013) 477–481.

[12] X. Sun, Y. Li, Colloidal carbon spheres and their core/shell structures with noble-metal nanoparticles, Angew. Chem. Int. Ed. 43 (2004) 597–601.

[13] B. Hu, K. Wang, L. Wu, S.H. Yu, M. Antonietti, M.M. Titirici, Engineering carbon materials from the hydrothermal carbonization process of biomass, Adv. Mater. 22 (2010) 813–828.

[14] D. Lozano-Castelló, J.M. Calo, D. Cazorla-Amorós, A. Linares-Solano, Carbon activation with koh as explored by temperature programmed techniques, and the effects of hydrogen, Carbon 45 (2007) 2529–2536.

[15] M. Karnan, K. Subramani, N. Sudhan, N. Ilayaraja, M. Sathish, Aloe vera derived activated high-surface-area carbon for flexible and high-energy supercapacitors, ACS Appl. Mater. Interfaces 8 (2016) 35191–35202.

[16] C. Zhang, L. Ren, X. Wang, T. Liu, Graphene oxide-assisted dispersion of pristine multiwalled carbon nanotubes in aqueous media, J. Phys. Chem. C 114 (2010) 11435–11440.

[17] J. Luo, L.J. Cote, V.C. Tung, A.T. Tan, P.E. Goins, J. Wu, et al., Graphene oxide nanocolloids, J. Am. Chem. Soc. 132 (2010) 17667–17669.
[18] L. Tian, M.J. Meziani, F. Lu, C.Y. Kong, L. Cao, T.J. Thorne, et al., Graphene oxides for homogeneous dispersion of carbon nanotubes, ACS Appl. Mater. Interfaces 2 (2010) 3217–3222.
[19] D.A. Dikin, S. Stankovich, E.J. Zimney, R.D. Piner, G.H. Dommett, G. Evmenenko, et al., Preparation and characterization of graphene oxide paper, Nature 448 (2007) 457–460.
[20] H.B. Yao, Z.H. Tan, H.Y. Fang, S.H. Yu, Artificial nacre-like bionanocomposite films from the self-assembly of chitosan-montmorillonite hybrid building blocks, Angew. Chem. Int. Ed. 49 (2010) 10127–10131.
[21] Q. Cheng, J. Duan, Q. Zhang, L. Jiang, Learning from nature: constructing integrated graphene-based artificial nacre, ACS Nano 9 (2015) 2231–2234.
[22] S. Gong, Q. Cheng, Bioinspired graphene-based nanocomposites via ionic interfacial interactions, Compos. Commun. 7 (2018) 16–22.
[23] Z. Zhang, J. Qu, Y. Feng, W. Feng, Assembly of graphene-aligned polymer composites for thermal conductive applications, Compos. Commun. 9 (2018) 33–41.
[24] S. Pei, J. Zhao, J. Du, W. Ren, H.-M. Cheng, Direct reduction of graphene oxide films into highly conductive and flexible graphene films by hydrohalic acids, Carbon 48 (2010) 4466–4474.
[25] J. Pampel, A. Mehmood, M. Antonietti, T.P. Fellinger, Ionothermal template transformations for preparation of tubular porous nitrogen doped carbons, Mater. Horiz. 4 (2017) 493–501.
[26] A.B. Fuertes, F. Pico, J.M. Rojo, Influence of pore structure on electric double-layer capacitance of template mesoporous carbons, J. Power Sources 133 (2004) 329–336.
[27] Z. Zhu, H. Jiang, S. Guo, Q. Cheng, Y. Hu, C. Li, Dual tuning of biomass-derived hierarchical carbon nanostructures for supercapacitors: the role of balanced meso/microporosity and graphene, Sci. Rep. 5 (2015) 15936.
[28] D. Zhang, M. Han, Y. Li, J. He, B. Wang, K. Wang, et al., Ultra-facile fabrication of phosphorus doped egg-like hierarchic porous carbon with superior supercapacitance performance by microwave irradiation combining with self-activation strategy, J. Power Sources 372 (2017) 260–269.
[29] Z. Zuo, T.Y. Kim, I. Kholmanov, H. Li, H. Chou, Y. Li, Ultra-light hierarchical graphene electrode for binder-free supercapacitors and lithium-ion battery anodes, Small 11 (2015) 4922–4930.